

Use of Simultaneous Seismic Facies Analysis in 4D Inversion Interpretation Workflow

Carlos Eduardo Borges de Salles Abreu, Alexandre Augusto Cardoso da Silva and Marcos Hexsel Grochau, Petrobras, Brazil, Edouard Jacquemin-Guillaume and Nathalie Lucet, Beicip-Franlab, France

Copyright 2011, SBGf - Sociedade Brasileira de Geofísica

This paper was prepared for presentation during the 12th International Congress of the Brazilian Geophysical Society held in Rio de Janeiro, Brazil, August 15-18, 2011.

Contents of this paper were reviewed by the Technical Committee of the 12th International Congress of the Brazilian Geophysical Society and do not necessarily represent any position of the SBGf, its officers or members. Electronic reproduction or storage of any part of this paper for commercial purposes without the written consent of the Brazilian Geophysical Society is prohibited.

Abstract

4D inversion results generally consist in cubes of property changes, such as differences in P-impedance (or P-velocity), in S-impedance (or S-velocity) and in density. A further step is to associate these elastic parameters to reservoir petrophysical parameters, such as porosity and absolute permeability, for fluid flow reservoir simulation purpose. Seismic facies analysis based on 4D inversion results is a key point to start addressing this demand. In this work, a pattern recognition approach, commonly used on the basis of 3D elastic inversion results, is extended to the 4D case. A unique pass is used to take into account both baseline and monitor information. By using this pattern recognition technique, variations of the seismic signature are identified, and related to possible 4D effects. A brand new seismic facies appears on the monitor data. This facies was interpreted thanks to the separation of pressure and saturation effect allowed by the use of P- and S-attributes. The resulting seismic facies maps fostered reservoir engineers to further analysis of pressure evolution in the reservoir.

Introduction

In the present work, monitor seismic data was acquired three months after the starting of water injection in the reservoir, and five months after the starting of oil production. When simple amplitude difference maps can reveal anisotropy in water displacement, and sealing or partially sealing faults, elastic parameters derived from 4D inversion should provide valuable insight to pressure and saturation changes inside the reservoir. This information can be used for reservoir simulation as well as for geomechanical modeling.

However, the combination of antagonists causes for Ip response (pressure drop due to depletion vs. gas liberation), the limitation of the seismic resolution at target level, the limited repeatability of the seismic data (obstruction by production platforms, different direction of shooting for monitor campaigns) dramatically increase the uncertainty on quantitative prediction. For this an interpretative method is here proposed.

A methodology for 4D multi-attribute interpretation is extended to 4D joint inversion results. Advantages in

considering a dataset of elastic parameters resulting from inversion are described. The general methodology for 4D multi-attribute segmentation is recalled, and the results of the seismic facies discrimination are then presented. To conclude, interpretation of the resulting seismic facies maps is provided, with a brief scenario of the possible changes occurred in the field.

Dataset description

The studied area corresponds to a deep-water offshore turbiditic field, located in Campos Basin, southeastern Brazilian continental shelf. The reservoir comprises a set of amalgamated poorly consolidated highly porous sandstones layers, with average thickness of 15m and embedded in encasing shales. Seismically detectable normal faults are observed in the area, with main strike direction almost parallel to the principal depositional direction (NW-SE), as shown in Figure 1.

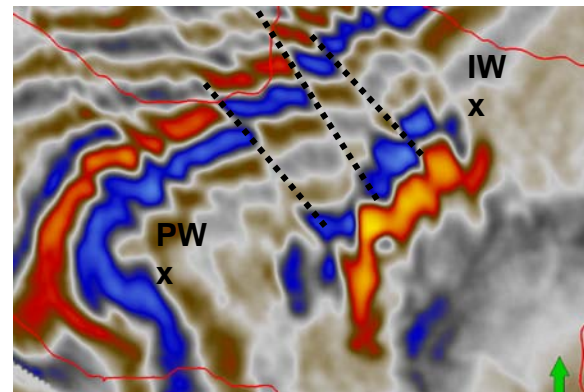


Figure 1 – A time-slice at target level from the baseline full-stack amplitude volume, where main faults are assigned as dotted lines. IW and PW are the well-heads from the injector and producer well...

A time-lapse study was carried out in the area, where the baseline and the monitor surveys were shot in 1999 and in 2004, respectively. Due to distinct acquisition parameters, where orthogonal shooting direction accounted for the main part, a simultaneous pre-stack cross-equalization processing was performed, to improve seismic repeatability and allow 4D interpretation. Another important factor on reducing seismic repeatability was operational obstacles in the area. Production platforms caused severe obstruction within the seismic survey during the monitor acquisition, impacting the underneath seismic illumination.

The dataset is composed of:

- Two wells respectively twins of Injector IW and Producer PW, with density, P- and S-impedance, porosity and Saturation.
- Two P- and two S-impedance cubes, derived from pre-stack 4D inversion of six high resolution PP seismic cubes, following the 4D inversion methodology developed by Tonellot et al. (2001).

Handling 4D Inversion results for characterization

A 4D joint seismic stratigraphic inversion, *i.e.*, a joint inversion of all angle stacks from both vintages was performed, disregarding any assumption on reservoir changes and correlated elastic parameters variation (see Delépine et al. (2010) for a methodology description on Sleipner case). As a model-based inversion technique, an *a priori* model is further updated in the seismic bandwidth with the seismic information during the inversion loop. The same initial model was used for the two vintages, given that the expected time differences due to production effects remain below one seismic sample. Figure 2 shows P-impedance maps corresponding to the lowermost part of the reservoir for both baseline and monitor vintages.

The pattern recognition method was used on P- and S-reflectivities obtained from the 4D joint inversion. As a matter of fact, elastic inversion allows improving the vertical resolution in acting as a stratigraphic deconvolution. Moreover, compared to original seismic data, inversion results present the advantage to be calibrated to the wells. Inversion process allows also getting rid of a significant part of the random noise affecting the observed seismic data. This random noise is rejected in the residuals cubes.

In this case, partial stacks from the two available vintages still presented severe time misalignment issue due to the orthogonal shooting between surveys. Furthermore, the vertical correction to apply varies with offset. After 4D joint inversion, which involved a realignment process during data pre-conditioning and a warping procedure, the P and S impedance cubes for all vintages are expressed in the same time basis. Seismic amplitude variations versus incidence angle due to 4D effects are directly integrated into the jointly inverted impedances.

Obviously, working on impedance-based attributes provides first hand information on the elastic variations occurred in the field during production phase.

4D Petroelastic variations

On a general basis, high pressure water injection in soft reservoir leads to pore-pressure increase in the well surroundings. As a matter of fact, an increase in pore-pressure boils down to a fall in effective pressure, a quantity often expressed as the difference of lithostatic and pore pressure. Velocity of the propagation media, and consequently impedance, is directly related to effective pressure. Basically, P (or S) impedance and effective pressure are varying in a proportionate way, on

exponential mode. A decrease in effective pressure would correspond to a decrease in P and S impedance value, the converse for increase case also being true. In addition, the replacement of light oil by brine water at the injector well would raise the P-impedance value of the reservoir rock, but let almost unchanged the S-impedance value. Water injection could thus have antagonist effects on P-impedance value in the reservoir. Nevertheless, this effect should be univocal on S-impedance, corresponding to a diminution of its value.

On the producer side, oil production in a closed system would lead to a pore pressure decrease at the producer well surroundings. This fall in pore pressure would lead to an effective pressure increase, and thus to a raise of P and S impedance value.

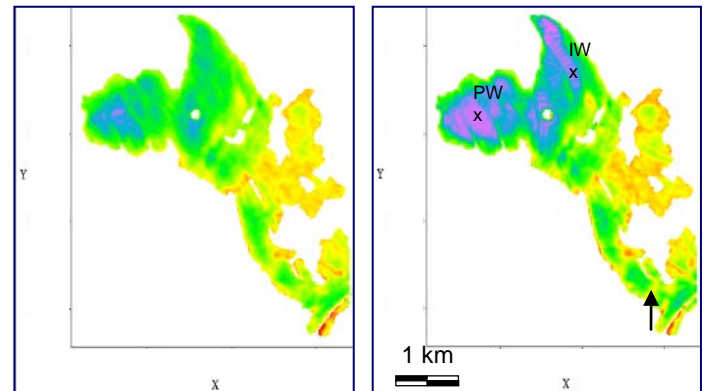


Figure 2 – P-Impedance maps at Top Reservoir horizon + 16 ms, for baseline (1999), on left image, and monitor (2004), on right image. The low values of impedance are in purple, high values in red. IW and PW indicate respectively the location of Injector and Producer wells. Note that no change appears between the vintages on the eastern part of the map.

4D Characterization by Simultaneous Seismic Facies Analysis

A simultaneous unsupervised seismic facies classification technique (Lucet and Fournier, 2001 and Abreu, 2008), was applied to separate seismic traces in different classes. This methodology is explained in Figure 3, where the classification is jointly done considering three time-lapse vintages (patent Fournier & Lucet, 2001). Three seismic facies are constituted on the set of attributes, which are the observed seismic data. Traces falling into green facies in baseline are classified also as green facies in the monitors. Magenta facies is present in baseline only and its traces fall into a blue facies in the monitors. Now considering a two vintages example and focusing on a particular bin, either the two traces baseline/monitor are classified into one single facies, or into two different facies. In the first case one may infer that the seismic signal remained steady from one year to

the other. In the other case, one infers from this change in the seismic signal possible changes inside the reservoir likely to be related to production.

In the present study, seismic facies classification is performed on P- and S-reflectivities resulting from 4D joint inversion. Seismic facies analysis based on elastic inversion results (Bertrand et al., 2002) is now extended to the case of multi-vintages characterization.

A 36ms window, corresponding to 10 samples, and comprising the entire reservoir interval as well as samples from the lower encasing shales was extracted from the P and S-reflectivity cubes, for the two vintages. P-reflectivity attributes from baseline are merged with monitor ones, and the seismic facies analysis will be run in this attribute space.

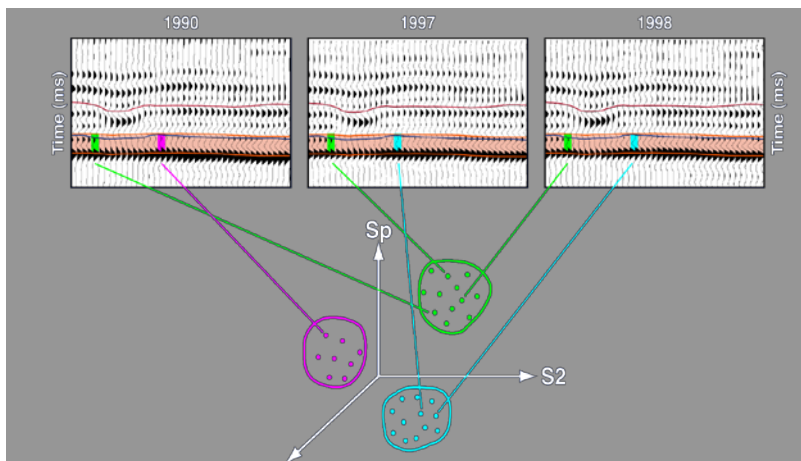


Figure 3 – Result of Discriminant analysis on a three-vintages example. Baseline was acquired in 1990, then a first monitor was shot in 1997 and a second in 1998.. (Lucet & Fournier, 2001)

Principles of the Seismic Facies Analysis

In the following, it is presented the basis of the 2D seismic facies analysis methodology, which is a pattern recognition technique that aims at classifying portions of traces extracted from the reservoir zone into seismic facies classes.

The workflow of this classification method is divided into three main steps: (i) a **multi-variate probability density function is estimated** in the space of attributes, by using the non-hierarchical method called K-nearest neighborhood. From the peaks of this probability density function is estimated the number of classes that can be seen in the dataset; (ii) for each defined class, a **learning trace is extracted** from the denser zones; and (iii) the learning traces are used in a **discriminant analysis**

process to generate the seismic facies map and its associated probability map.

As it is based on Bayesian formalism, the discriminant analysis tool conveys the segmentation results in a probabilistic frame.

Uncertainties can be thus quantified by computing the probabilities to assign each seismic trace portion to the different facies (Déquirez et al., 1995). Each trace will consequently be assigned to the facies with the highest probability value. This point and the possibility of a clear determination of the number of classes make this approach of particular interest compared to the classical ones.

Each seismic facies corresponds to a particular shape of seismic trace, which may lead to interpretation in terms of band-limited seismic response to distinct geological features.

In the case study, the previously described unsupervised approach was implemented, and tackled the issue of the production effects interpretation with the most neutral starting point.

Discrimination results

A probability density function is calculated on the merged dataset, leading to the detection of four distinct seismic facies. A non-parametric approach was selected; as a consequence, no Gaussian assumption is used to describe the class distributions in the attribute space. Clusters delineation this way can fit with the actual data structure. Four seismic facies were delineated on P-reflectivity multi-vintage dataset classification, and, as both vintages are classified in a single pass, the seismic facies definition is unique. It is noticeable that, as shown in Figure 4A, no traces fall into the fourth facies, coded in yellow colour, in the baseline survey. The resulting facies map for the baseline survey presents only three facies: a light blue facies at the external part of reservoir area; a green facies corresponding to internal sand deposits; and lastly, a red facies, possibly calling for local variations of the sands quality or thickness. A maximum thickness of 25m sandstone has already been vertically drilled in this reservoir, and due to sedimentary pinch-out of the reservoir, lateral variations of thickness are expected. Limited vertical resolution makes this thickness variation difficult to settle on a seismic interpretation basis.

Besides the previously detected three facies, the monitor survey map exhibits a fourth one, located in the area of producer and injector wells.

Comparing Figures 4A and 4B, the light blue and the green facies are keeping the same site from baseline to monitor map. Conversely, the red facies noticeably sprawls on the northern part of the reservoir, in the monitor map, on the right.

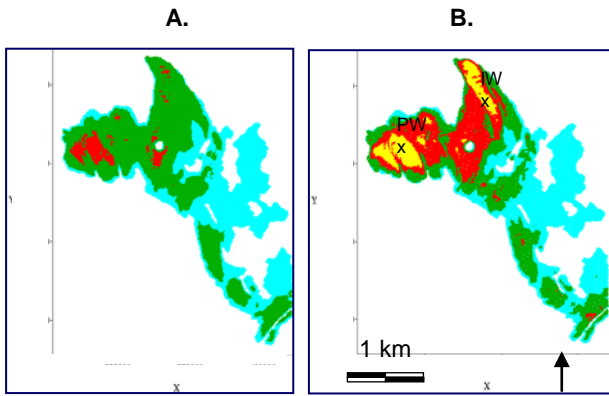


Figure 4 – Seismic facies maps from unsupervised analysis using attributes from P-reflectivity, for A., baseline (1999) and B., monitor (end of 2004).

Then the same segmentation process was applied to S-reflectivity attributes. The multi-vintage S dataset was classified into four seismic facies, this number of facies being given by the probability density function. Figure 5 presents the facies map obtained for baseline with S-reflectivity attributes. Three only on the four facies show up for baseline, as it is observed on P-attributes (Figure 5A). The green facies is the most frequent one whereas the red one is the sparser. The spatial distribution of these three facies presents an aspect of stripes in the northern region. The stripes seem to stress the faults that we know to divide the reservoir (Figure 1).

Again, the fourth facies (yellow) is present on the monitor map only. Note that no direct link exists between the seismic facies code for P and S dataset, the analysis having been conducted sequentially. However a similar colour coding was kept. As a general observation on the S- seismic facies maps, light blue facies area diminishes, when green facies extends from baseline to monitor. Outside northern part the area of light blue facies appears too scattered to be representative of any geological local variation. The red facies area for S-results is considerably spreading on monitor year. Some traces of the producer area lining the fault are falling into the yellow facies, yet this facies is mainly concentrated in injector area.

On P seismic facies maps for monitor year the yellow facies appears in injector as well as in producer area. This fourth facies standing out on monitor year gives insight of a facies change in the area of injector, which will be visible together by P and S elastic parameter. A similar facies change seems to happen in the producer area, but this time not detected by S parameter.

Note that classifications run on P- as on S-results show high associated probability of good assignment in the northern part of the reservoir (above 0.9).

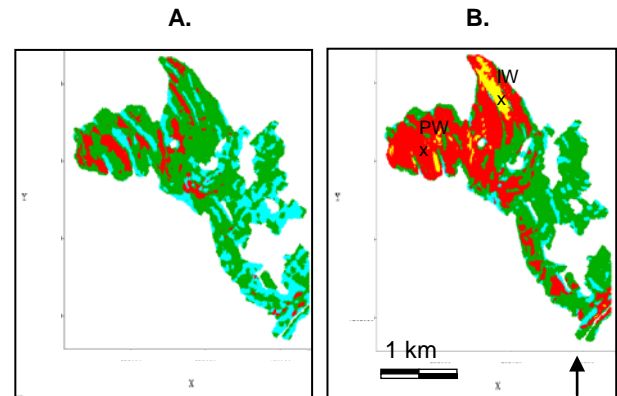


Figure 5 – Seismic facies maps from unsupervised analysis using attributes from S-reflectivity, for A., baseline (1999) and B., monitor (2004).

To explore the nature of the seismic facies changes, the comparison of characteristic traces for each cluster proved relevant. Characteristic traces are the ones whose classification was most successful, for this they are regarded as typical of their seismic facies (Figure 6 & 7).

For every P- characteristic trace, the first seismic sample shows a negative value. This negative reflectivity corresponds to the seismic trough observed at the top of the lower impedance sands. Then a positive peak indicates the positive impedance contrast at the reservoir base (Figure 6&7). It has to be stressed that the vertical resolution of the reservoir cannot be fully achieved due to the limited frequency range of seismic signal, with a mode at 30 Hz for $V_p = 2700 \text{ m.s}^{-1}$ in reservoir.

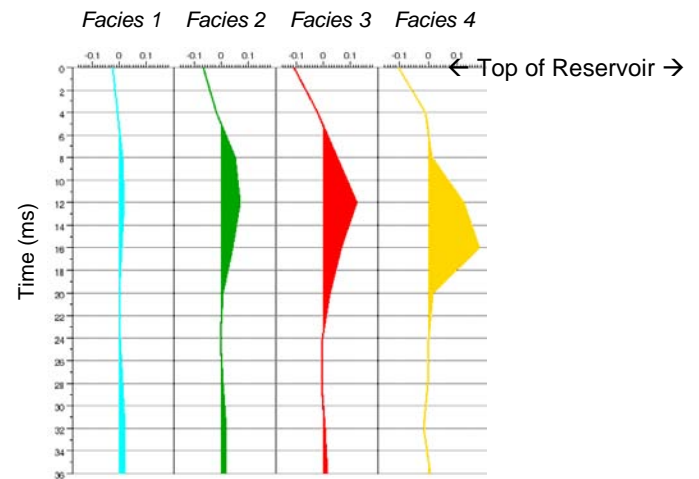


Figure 6 - Characteristic traces of the four seismic facies obtained for the multi-vintages discriminant analysis performed on P dataset.

Observing the pattern of the characteristic traces on P-reflectivity results, we notice that the positive peak is very flattened for the light blue facies, visible on the green

facies, and still more marked on red facies. The yellow facies, present on monitor year only, is characterized by a still stronger positive peak, moreover positively shifted (+ 4 ms). As shown by the Figure 7, the behavior for S-reflectivity typical traces is similar.

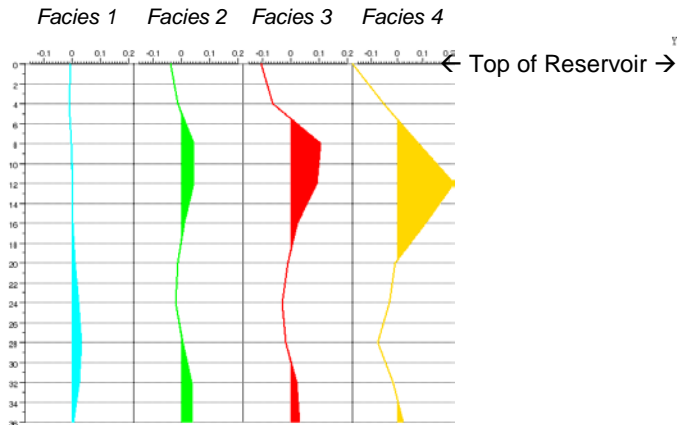


Figure 7 – Characteristic traces of the four seismic facies obtained for the multi-vintages seismic facies analysis performed on S dataset.

Still on P-reflectivity basis and in order to insure of the seismic repeatability, we performed a seismic facies analysis 200 ms above the Top Reservoir. As illustrated by Figure 8, no relevant difference appears between the seismic facies maps of different vintage, which validates the methodology.

Interpretation

From the characteristic traces and the seismic facies maps we propose to interpret the light blue facies as a thin or absent reservoir facies. We interpret the green facies as corresponding to an average thick sand facies. In this block of 15 sq. kilometers area, and based on the available two wells logs, no lateral variation of texture nor porosity is expected. For this reason the interpretation of the red facies is more ambiguous. The red areas on the baseline map could correspond to thicker sands. However its extension grows noticeably on the monitor. This inflation could be related to the strong pressure increase raised by injector (IW). The yellow facies appearing both at producer and injector area on P-results could be related to production effects. Indeed it does not appear in baseline seismic facies map. The strengthened reflectivity peak observed on the characteristic trace announces a higher impedance contrast at base of reservoir, that is to say a still lower value of impedance inside the reservoir. The observed positive time shift of this peak may be explained by a velocity decrease inside reservoir, coherent with impedance decrease.

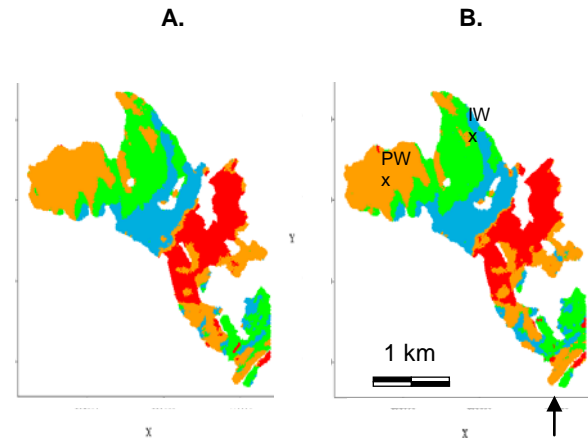


Figure 8 – Seismic facies maps realized 200 ms above the Top Reservoir on P-reflectivity attributes, with a 10 seismic samples window, for A., baseline and B., monitor. No noticeable differences are observed between 1999 and 2004 seismic facies distribution.

The injection at IW started three months before the acquisition of the monitor. The production started at W2, five months before acquisition of the monitor. Note that an overpressure episode occurred at IW induced a peak of the PDG pressure measurement few weeks before monitor shooting. The red facies development could correspond to a general increase of pore pressure within the block. Stronger pore pressure increase may be traced out by yellow facies in northeastern area. From pressure history curves, measured by PDG gauges on injector and producer, it can be seen that the pressure increase from IW did not hold the pressure state at PW, which depleted. Fast depletion, bubble point close from the original pressure in reservoir and good quality oil (28° API) could have induced gas liberation at PW. Hence the presence of yellow facies on P- seismic facies map at PW location might be explained by gas. This hypothesis is coherent with the S-attributes not detecting the fluid changes. Note that at injector well, substitution of oil by water could have tightened reservoir sands. However the amount of injected water may have been too limited after three months injecting to balance the overpressure effect.

The characteristic traces of S-reflectivity show a very similar pattern to the P- characteristic traces (Figure 7). Their interpretation is therefore identical, except that in this case effective pressure decrease is the main reason to explain the S-impedance fall.

The gas liberation at producer well had not been considered by the fluid flow reservoir simulation before this work. Yet it was no surprise to the asset engineer which confirmed a neat increase of Gas-oil-ratio value. The sealing fault lining the injector area was not included into the geological model before this work. After considering the sealing fault, the engineer dramatically improved the history matching of pressure.

Conclusions

On the basis of a 4D joint inversion integrating all angle stacks, all vintages together with well data and horizon picking, a seismic facies analysis has pointed effective pressure changes and possible gas liberation. Seismic facies analysis was conducted separately on P- and S-reflectivity attributes, generating two sets of seismic facies maps. S-attribute offered a valuable contribution to the analysis of injection impact on the pressure state change, when P-attribute allowed evidencing gas liberation at producer well. Quite surprisingly no cluster was formed which isolate gas effect and pressure effect but the two responses fell into the same group. No assumption on the elastic properties change due to field operations was made at any prior stage. Cluster segmentation issue was addressed by unsupervised approach, which offers the most objective way to data classification. Hence the used classification is from the most neutral kind. Interpretation of these seismic facies maps called for three hypotheses: a. a dominant effect of effective pressure fall on water substitution at injector place, b. a sealing fault lining the injector area, c. a fast depletion followed by gas liberation at producer place. As an interpretative method, this seismic reservoir characterization proved useful to elaborate scenarios which enable improvement of the history matching of the field dynamic measurements. A supervised analysis using the typical response of gas substitution and fall of effective pressure for guiding the classification would constitute a complementary approach. These typical responses could be obtained thanks to a modeling at wells based on quantitative curves of saturations and porosities for fluid effect, and laboratory measurements for pressure effect.

Acknowledgments

The authors express many thanks to Petrobras for permission to publish these results. The authors thank João Paulo Pereira Nunes, Luis Carlos de Sousa Junior, Alvaro Favinha Martini, and all colleagues from Marlim Sul Asset Team for fruitful technical discussions, as well as Nicolas Delépine, Vincent Clochard and Michel Léger, from IFP Énergies Nouvelles, and Gaël Lecante from Beicip-Franlab.

References

Abreu, C.E.B.S., 2008. Time-lapse (4D) Seismic Interpretation Methodologies based on Kriging Analysis: Application to the SENLAC (Onshore Canada) and Marlim (Offshore Brazil) Heavyoil Fields. PhD Thesis. Université Nancy, 375pp.

Bertrand, C., Tonellot, T. and Fournier, F., 2002, Seismic facies analysis applied to P and S impedances from pre-stack inversion, 72nd Ann. Internal. Mtg., Soc. Expl. Geophys., Expanded Abstracts, 217-220.

Delépine, N., Labat, K., Clochard, V., Ricarte, P. and Le Bras, C., 2010, 4D Joint pre-stack seismic stratigraphic inversion of the Sleipner-CO2 case: 72nd EAGE Conference & Exhibition, Extended Abstracts.

Déquirez, P.-Y., Fournier, F., Blanchet, C., Feuchtwanger, T. and Torriero, D., 1995, Integrated stratigraphic and lithologic interpretation of the East-Senlac heavy oil pool, 65th Annual SEG Meeting Expanded Abstracts, 104-107.

Fournier, F., Déquirez, P.-Y., Macrides, C.G., Rademakers, M., Quantitative lithostratigraphic interpretation of seismic data for characterization of the Unayzah Formation in central Saudi Arabia, Geophysics, Vol. 67, No. 5 (September-October 2002); 1372-1381.

Fournier, F., Lucet, N., 2001, Méthode pour faciliter le suivi au cours du temps de l'évolution d'une zone souterraine par analyse comparée de différents jeux d'enregistrements sismiques. Brevet EN 01/05.675 n° 2.824.147 (France, 27/04/01), Brevet US (Etats-Unis, 22/04/02, n° de dépôt 126.605)

Lucet, N., Fournier, F., 2001, 4D data interpretation through seismic facies analysis, *In* SEG - 71st Annual International Meeting of the Society of Exploration Geophysicists, San Antonio, Sept. 9-14 2001, Expanded Abstracts, 1640-1643.

Tonellot, T., Macé, D., Richard, V., 2001, Joint stratigraphic inversion of angle-limited stacks. 71st SEG Annual International Meeting, Expanded Abstracts, p.227-230.